J Math Chem
DOI 10.1007/s10910-016-0689-5

REVIEW

The computation of radial integrals with nonclassical quadratures for quantum chemistry and other applications

Bernie D. Shizgal[1] · **Nicholas Ho**[2] · **Xingwei Yang**[3]

Received: 22 August 2016 / Accepted: 16 September 2016

Abstract The computation of radial integrals on the semi-infinite axis is an important computationally intensive feature of quantum chemistry computer codes with additional applications to physics and engineering. There have been numerous algorithms proposed to evaluate these integrals efficiently. Many of these approaches involve the transformation of the semi-infinite axis, $r \in [0, \infty)$, to the finite interval, $x \in [-1, 1]$, and the use of the Gauss–Legendre or Gauss–Chebyshev quadratures to evaluate the integrals. These mappings redistribute the quadrature points in many different ways. The approach in this paper is to compute the radial integrals with the Gauss–Maxwell nonclassical quadrature defined by the weight function $w(r) = r^2 e^{-r^2}$ appropriate for the semi-infinite interval and to also use scaling of the quadrature points. We carry out numerical experiments with simple model radial integrands and compare with the results of previous workers.

Keywords Radial integrals · Quadratures · Mappings · Gauss–Maxwell quadrature

1 Introduction

Quantum chemistry computer codes whether based on density functional theory [11,32,39] or otherwise require the efficient numerical evaluation of three dimensional integrals in spherical polar coordinates [4]. The angular portion of the integrals

✉ Bernie D. Shizgal
shizgal@chem.ubc.ca

1 Department of Chemistry, University of British Columbia, Vancouver, Canada

2 Department of Computer Science, University of British Columbia, Vancouver, Canada

3 Department of Mathematics, University of British Columbia, Vancouver, Canada

Published online: 27 September 2016

are often evaluated with Lebedev quadratures [10,17,22]. The efficient evaluation of the remaining radial integral between Gaussian basis functions is an ongoing activity in the quantum chemistry community. Several reviews have been published that discuss the variety of current methods [11,26,28,30]. There have been numerous studies concerning the radial integrals based on model functions that mimic the anticipated forms of the radial integrals and there have been a series of numerical experiments reported [1,24,25,38].

These authors have used model radial integrands which exhibit two and three maxima such as the sum of simple Gaussians of the form

$$F_2(r) = r^2\left[e^{-r^2} + 10e^{-10r^2}\right], \quad r \in [0, \infty),$$

and

$$F_3(r) = r^2\left[e^{-r^2} + 10e^{-10r^2} + 100e^{-100r^2}\right]. \tag{1}$$

The authors employed different transformations from the semifinite interval to the finite interval $x \in [-1, 1]$ and then used either Gauss–Legendre [27] or Gauss–Chebyshev quadratures [16] to evaluate the integral

$$I = \int_0^\infty F(r)dr, \tag{2}$$

as

$$I = \int_{-1}^{1} F[r(x)]r'(x)dx, \tag{3}$$

with $F(r) = F_2(r)$ or $F(r) = F_3(r)$ and a variety of transformations $r(x)$ [24,25,27,29,38]. A comparison of these methods were reported by Gill and Chien [7], El-Sherbiny and Poirier [6] and Mitani [22]. These transformations from r to x redistribute the quadrature points in different ways and the efficiency of the procedures depends on the manner in which the grids capture the redefined integrands [7]. Boyd [2,3] has discussed in detail the convergence of integrals defined on the semi-infinite interval and evaluated with such transformations. There have also been some reports on the analytical evaluation of these radial integrals [20,23].

Gill and Chien [7] have proposed a new nonclassical quadrature for the evaluation of these integrals with a comparison of the different mappings that were used previously. Kakhiani et al. [12] do not treat the full half infinite interval and instead use an adaptive radial quadrature grid that relies on subdividing the radial interval as defined by the maxima and minima of the integrands. This method is not paticularly adapted to the numerical evaluation of numerous integrals with different integrands. Lindh et al. [18] compared the different schemes noted previously using a simple Gaussian orbital normalized according to

$$\frac{2\alpha^{(\ell+3)/2}}{\Gamma[(\ell+3)/2]}\int_0^\infty r^{\ell+2}e^{-\alpha r^2}dr = 1. \tag{4}$$

This integral can be evaluated exactly with a small number of the Gauss–Maxwell quadratures [33,36,37] and the appropriate scale change as discussed in Shizgal [35]; see Fig. 3.5. The objectives of the current paper is to consider alternate model integrands and demonstrate the convergence of the scaled Gauss–Maxwell quadrature [33] in the evaluation of these radial integrals. A comparison is also provided with the change of variable from $r \in [0, \infty)$ to $x \in [-1, 1]$. It is important to mention the use of the nonclassical Rys quadrature for the evaluation of integrals in quantum chemistry [5,15,19,34].

2 Nonclassical Gaussian quadratures for model radial integrals

In addition to $F_3(r)$, Eq. (1), used by previous workers [1,7,24,25,38], we consider similar integrands defined by,

$$F_a(r) = r^2\left[20e^{-(r-1)^2} + 3e^{-(r-3)^2} + 0.5e^{-(r-5)^2}\right], \tag{5}$$

$$F_b(r) = r^2\left[60e^{-2(r-0.5)^2} + 4e^{-(r-2)^2} + 0.8e^{-(r-4)^2}\right]. \tag{6}$$

which exhibit a larger radial range than $F_3(r)$. These are compared in Fig. 1. We consider the numerical integration of the integral given by Eq. (2) and the three integrands, Eqs. (1), (5) and (6) with the Gauss–Maxwell quadrature [33], defined by

$$I_{GM} = \int_0^\infty r^2 e^{-r^2} g(r) dr,$$
$$\approx \sum_{n=1}^{N} w_i g(x_i). \tag{7}$$

The quadrature points, x_i and weights, w_i, are calculated with the Gautsche–Stieltjes procedure as described elsewhere [35]. An important feature of the quadrature is the

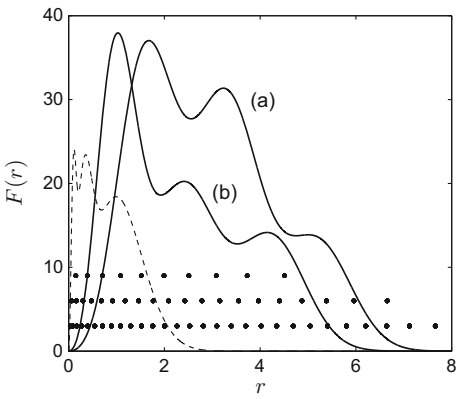

Fig. 1 Variation of the integrands with the dashed line representing $50F_3(r)$ given by Eq. (1) and (*a*) $F_a(r)$ given by Eq. (5) and (*b*) $F_b(r)$ given by Eq. (6). The Gauss–Maxwell quadrature points with $w(x) = x^2\exp(-x^2)$ with N = 10, 20 and 30 are shown by the *solid symbols*

scaling of the points and weights so as to redistribute the quadrature points and achieve convergence.

Thus, given an integral of the form

$$I = \int_0^\infty F(r)dr, \tag{8}$$

the variable r can be scaled, that is $r = sx$, so that

$$\begin{aligned} I(s) &= s\int_0^\infty F(sx)dx, \\ &= s\int_0^\infty x^2 e^{-x^2}\frac{F(sx)}{x^2e^{-x^2}}dx, \\ &\approx \sum_{i=1}^{N} W_i F(sx_i), \end{aligned} \tag{9}$$

where the so-called big weights are defined as

$$W_i = \frac{sw_i}{x_i^2 e^{-x_i^2}}. \tag{10}$$

Also shown in Fig. 1 by the solid symbols are the unscaled positions of the Gauss–Maxwell quadrature points for $N = 10$, 20 and 30. It is important to note the coverage of the integrands by the quadrature points which can be redistributed with the scaling factor s. The convergence of the integral, Eq. (2), with the three integrands given by Eqs. (1), (5) and (6) versus N for several scaling factors, s are shown in Fig. 2. The convergence for $F_a(r)$ and $F_b(r)$ shown in Fig. 2a, b, respectively, are very similar with the relative error of the order of 10^{-10} with 16–20 quadrature points and a sufficiently large scaling factor to move the quadrature points to larger radial distances. The errors for the integration of $F_3(r)$, Eq. (1), are not as small with scaling factors less than 1 in order to move the quadrature points inwards to smaller radial distances. There does not appear to be a rigorous mathematical analysis of the role of the scaling factor. There have also been several discussions of the use of Gaussian functions as basis functions and their associated quadratures [13,14,21]. However, even if these can be suitably adapted for particular integrals, the computational time could be high.

3 Transformations from the semi-infinite axis to $x \in [-1, 1]$

There have been numerous discussions concerning the evaluation of integrals on the semi-infinite interval with the transformation of $r \in [0, \infty)$ to $x \in [-1, 1]$ and the use of Gauss–Legendre [27] or Gauss–Chebyshev [16] quadrature points. Gottlieb and Orszag [8] suggested that the Laguerre and Hermite polynomials have poor resolution properties when used as basis functions for the expansion of $\sin(x)$ and as a consequence these basis functions will not be of practical value for spectral methods. Grosch

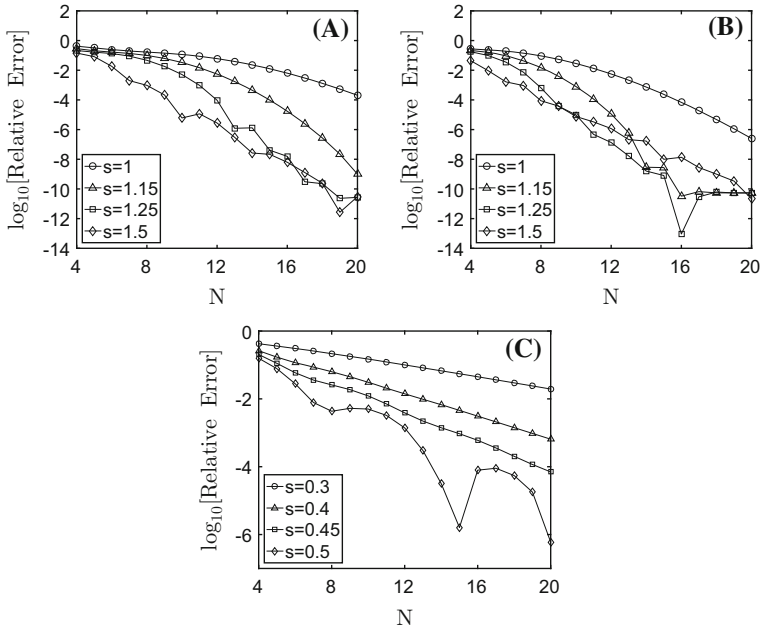

Fig. 2 Convergence of the integrals versus the number of Gauss–Maxwell quadrature points, N, in terms of the Relative Error $= |1 - I_{approx}/I_{exact}|$ for different scale factors, s, for **a** $F_a(r)$, Eq. (5), **b** $F_b(r)$, Eq. (6) and **c** $F_3(r)$, Eq. (1)

and Orszag [9] considered the solutions for six different problems such as Burger's equation, the Falkner–Skan equation and other problems by either truncating the infinite domain or with suitable mappings and then use Chebyshev polynomials. Boyd [2] provided a detailed mathematical analysis of the different mappings and concluded that algebraic mappings are preferred over exponential mappings. A detailed mathematical analysis of the use of mappings for spectral methods in unbounded domains was also presented by Shen and Wang [31].

In each application, the motive to transform the problems to $x \in [-1, 1]$ is to then be able to use Chebyshev or Legendre quadratures as a grid in a pseudospectral calculation. This is analogous to the use of mappings in the evaluation of radial integrals defined on $r \in [0, \infty)$ and transformed to integrals over $x \in [-1, 1]$. It should be noted that the solution of the Schrödinger equation for the harmonic oscillator on the infinite axis is best accomplished with the Hermite polynomials as basis functions, as these are the eigenfunctions. The Laguerre polynomials are the eigenfunctions of the radial differential equation for the hydrogen atom.

In the context of the numerical evaluation of radial integrals, we propose to use quadratures that are defined on the semi-infinite axis. There have been numerous alternate choices in the literature for the transformation of the semi-infinite axis to the finite interval, $x \in [-1, 1]$. These transformations were summarized previously [6,7] and are also reproduced in Table 1 from [35]. The use of a quadrature defined on the semi-infinite axis is best illustrated with the radial integral considered by Lindh et

Table 1 Different mappings of the semi-infinite interval $r \in [0, \infty)$ to $x \in [-1, 1]$

References	Mapping
Boyd [2]; Treutler and Ahlrichs [38]	$x = 1 - 2e^{-r/s}$
Murray et al. [25]	$x = 2\sqrt{1 - e^{-r/s}} - 1$
Boyd [3]; Becke [1]	$x = \frac{r-s}{r+s}$
Mura and Knowles [24]	$x = 2\sqrt{r/(r-s)} - 1$

The parameter s is a scaling factor

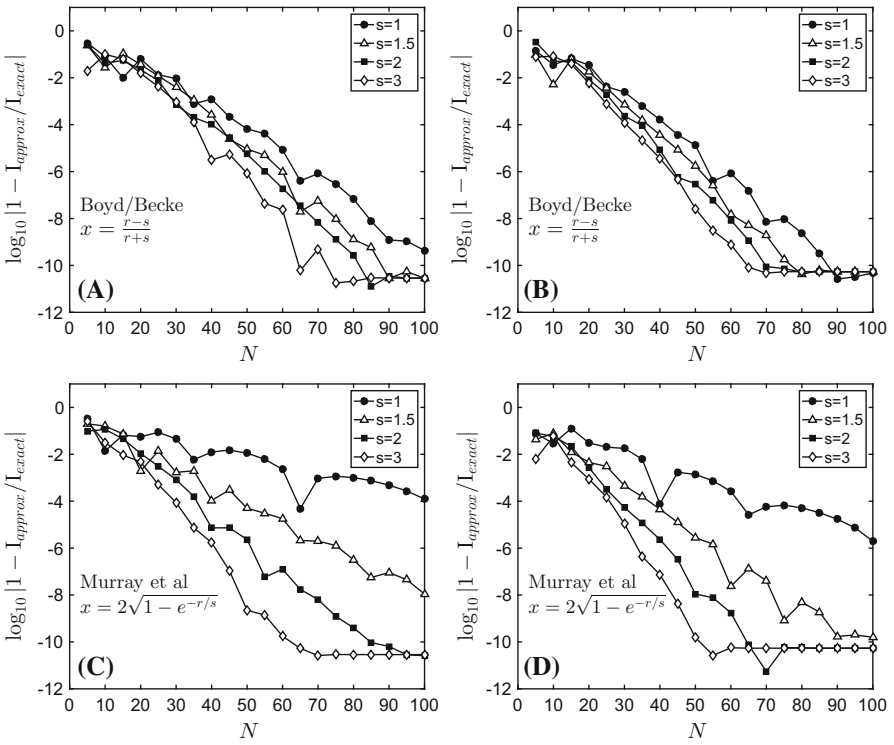

Fig. 3 Convergence of the integrals versus the number of Gauss–Legendre quadrature points, N, for different scale factors, s, with the different transformations from $r \in [0, \infty)$ to $x \in [-1, 1]$ as shown and discussed in the text. For **a**, **c** $F_a(r)$, Eq. (5). For **b**, **d** $F_b(r)$, Eq. (6)

al. [18], Eq. (4). They carried out a detailed comparison of the mappings in Table 1 applied to this integral. In the first instance, they considered a comparison of all four mappings for $\ell = 0$ with 50, 200 and 500 quadrature points, their Fig. 2, and also for different ℓ values with $N = 100$, their Fig. 3. In each case, machine accuracy could be achieved with a sufficiently large number of quadrature points.

However, the exact evaluation of this integral with the Gauss–Maxwell quadrature is obtained for $s = 1/\sqrt{\alpha}$ with $N = 4, 5, 6$ and 8 quadrature points for $\ell = 6, 8, 10$ and 14, respectively; see Fig. 3.5 in [35]. Lindh et al. [18] evaluated the integral in Eq. (4) with the transformations in Table 1 which do not provide similar exact results. They also proposed a nonclassical quadrature based on the weight function, $w(x) = \ln^2(x)$,

$x \in [-1, 1]$, referred to as the MultiExp quadrature. A comparison of this quadrature with the scaled Gauss–Maxwell quadrature for $F_3(r)$ was reported previously [35]; see Table 3.3.

The convergence versus N of the radial integral, I, Eq. (2), with the scaled Gauss–Maxwell quadrature for each radial integrand, Eqs. (1), (5) and (6), is shown in Fig. 2. It is clear that an increase in the scaling factor, s, improves the convergence in Fig. 2a, b so that the error is of the order of 10^{-10} with N = 16–20. For $F_3(r)$ in Fig. 2c, the error is of the order of 10^{-6} with N = 20 for the largest scaling factor chosen.

The radial integrals with $F_a(r)$, Eq. (5), and $F_b(r)$, Eq. (6), were evaluated with the Gauss–Legendre quadrature with the transformation by Boyd [3] and Becke [1]. The convergence is shown in Fig. 3a, b, respectively, for different scale factors. Of the order of 60–70 quadrature points are required to achieve an error of the order of 10^{-10} with a sufficient scaling of the quadrature points. The scaling of the quadrature points does not appear to drastically change the rate of convergence except for the largest N values of 60–100.

The convergence with the Murray et al. [25] transformation is shown in Fig. 3c, d. For these, the scaling provides a bigger improvement in the convergence than for the Boyd/Becke transformation [1–3] in Fig. 3a, b, respectively. With a scale factor, s = 3, the error of 10^{-10} is achieved with 50–60 quadrature points, marginally better than for the Boyd/Becke transform. The results for the different radial integrands, $F_a(r)$, Eq. (5) and $F_b(r)$, Eq. (6) are very similar.

The convergence with the exponential transformation shown in Fig. 4a, b exhibits a very strong dependence on the scale factor, s. The error is of the order of 10^{-10} with approximately 40 quadrature points with s = 3. By contrast, the transformation by Mura and Knowles [24] shown in Fig. 4c, d does not provide the same rate of convergence even with scaling. The error of 10^{-10} is achieved with approximately 80–100 quadrature points for both integrands. A comparison of the results in Figs. 3 and 4 with those in Fig. 2 shows that the Gauss–Maxwell quadrature on the semi-infinite interval is superior to the other algorithms which involve the transformation to the interval $x \in [-1, 1]$.

To better understand the role of the transformations for $r \in [0, \infty)$ to $x \in [-1, 1]$ Gill and Chien [7] showed in their Fig. 1 the r_i nodes versus x_i quadrature points for six different transformations to illustrate the manner in which the points are distributed in the interval $[-1, 1]$. However, it is instructive to show the radial functions $F_a[x(r)]$, Eq. (5), with the exponential mapping, and $F_b[x(r)]$, Eq. (6) for the mapping by Mura and Knowles [24] versus x in Fig. 5. In both figures, the distribution of quadrature points, shown by the solid symbols for N = 10, 20 and 30, respectively, is denser at the ends of the intervals, that is near $r = 0$ and $r \to \infty$, where the integrands tend to zero. In Fig. 5a, the second peak of $F_a(r)$ clearly shown in Fig. 1a is too close to the boundary at x = 1 to be resolved. It is clear that the convergence of the radial integrals with the Gauss–Maxwell quadrature is superior to the methods that rely on the transformation to $x \in [-1, 1]$ and the use of Gauss–Legendre or Gauss–Chebyshev quadrature points.

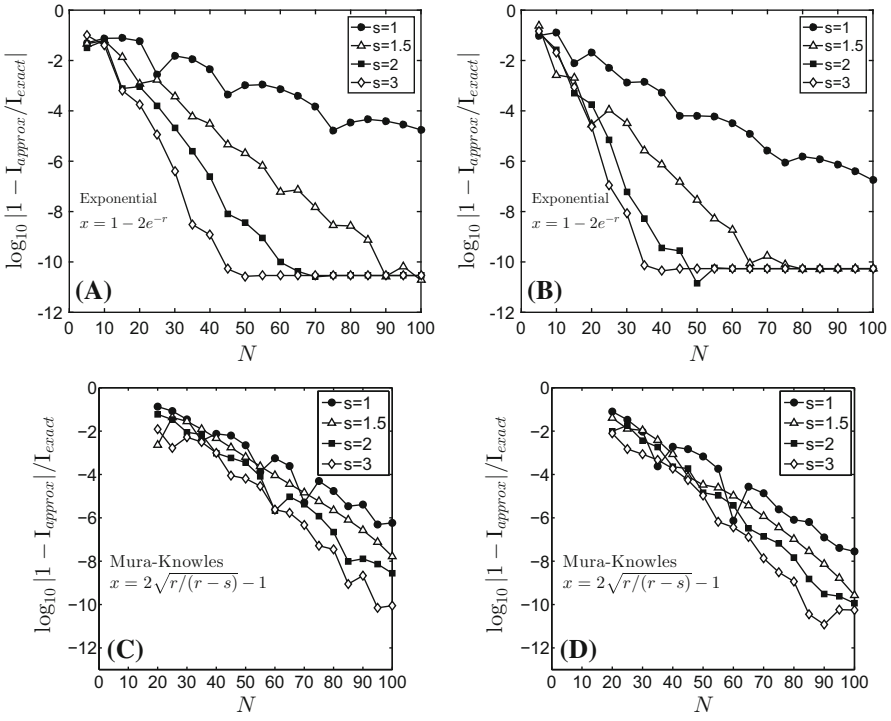

Fig. 4 Convergence of the integrals versus the number of Gauss–Legendre quadrature points, N, for different scale factors, s, with the different transformations from $r \in [0, \infty)$ to $x \in [-1, 1]$ as shown and discussed in the text. For **a**, **c** $F_a(r)$, Eq. (5). For **b**, **d** $F_b(r)$, Eq. (6)

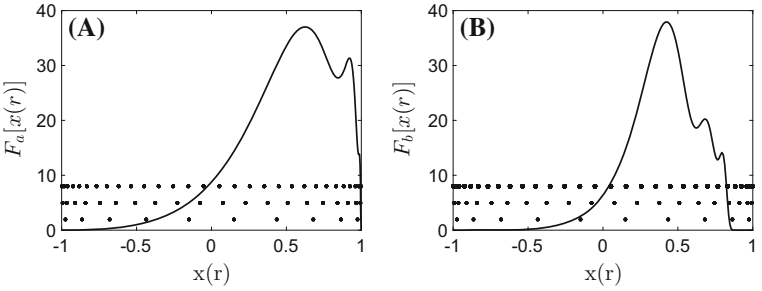

Fig. 5 The variation of the radial integrands, $F_a[x(r)]$, versus $x(r), x \in [-1, 1]$ for the exponential mapping [2,38] and $F_b[x(r)]$ for the mapping by Mura and Knowles [24]. The *symbols* along the x-axis are the quadrature points for $N = 10$, 20 and 30, respectively, to show the distribution of quadrature points as N increases

4 Summary

A comparison of different quadrature procedures for the evaluation of model radial integrals was presented. A Gauss–Maxwell quadrature based on the weight function, $w(x) = x^2 e^{-x^2}, x \in [0, \infty]$ used previously in kinetic theory applications [33,36,

37] was introduced and compared with the Gauss–Legendre or Gauss–Chebyshev quadratures on $x \in [-1, 1]$ with different transformations, $r(x)$ was considered. An important aspect of all the methods is to appropriately scale the quadrature points so as to improve the convergence. The Gauss–Maxwell quadrature appears to have provided the most accurate evaluation of the model integrands studied. The transformations to the finite interval $x \in [-1, 1]$ redistribute the Legendre and/or Chebyshev quadrature points in a manner that does not necessarily cover the range of the integrands on the new interval. Work is in progress to consider alternate weight functions on the semi-infinite interval to improve upon the results with the Gauss–Maxwell quadrature.

References

1. A.D. Becke, A multicenter numerical integration scheme for polyatomic molecules. J. Chem. Phys. **88**, 2547–2553 (1988)
2. J.P. Boyd, The optimization of convergence for Chebyshev polynomial methods in an unbounded domain. J. Comput. Phys. **45**, 43–79 (1982)
3. J.P. Boyd, Exponentially convergent Fourier–Chebyshev quadrature schemes on bounded and infinite domains. J. Sci. Comput. **3**, 99–109 (1987)
4. S. Choi, K. Hong, J. Kim, W.Y. Kim, Accuracy of Lagrange-sinc functions as a basis set for electronic structure calculations in atoms and molecules. J. Chem. Phys. **142**, 094116 (2015)
5. M. Dupuis, A. Marquez, The Rys quadrature revisited: a novel formulation for the efficient computation of electron repulsion integrals over Gaussian functions. J. Chem. Phys. **114**, 2067–2078 (2001)
6. A. El-Sherbiny, R.A. Poirier, An evaluation of the radial part of the numerical integration commonly used in DFT. J. Comput. Chem. **25**, 1378–1384 (2004)
7. P.M.W. Gill, S.-H. Chien, Radial quadrature for multiexponential integrands. J. Comput. Chem. **24**, 732–740 (2003)
8. D. Gottlieb, S. Orszag, *Numerical Analysis of Spectral Methods: Theory and Applications* (SIAM, Philadelphia, 1977)
9. C.E. Grosch, S.A.A. Orszag, Numerical solution of problems in unbounded regions: coordinate transforms. J. Comput. Phys. **25**, 273–295 (1977)
10. D.J. Haxton, Lebedev discrete variable representation. J. Phys. B At. Mol. Opt. Phys. **40**, 4443–4451 (2007)
11. T. Helgaker, P. Jorgensen, J. Olsen, *Molecular Electronic Structure Theory* (Wiley, New York, 2000)
12. K. Kakhiani, K. Tsereteli, P. Tsereteli, A program to generate a basis set adaptive radial quadrature grid for density functional theory. Comput. Phys. Commun. **180**, 256–268 (2009)
13. H. Karabulut, M. Kalay, Distributed Gaussian discrete variable method. Int. J. Quant. Chem. **104**, 16–28 (2005)
14. H. Karabulut, E.L.I. Sibert, Distributed Gaussian polynomials and associated quadratures. J. Math. Phys. **38**, 4815–4831 (1997)
15. H.F. King, M. Dupuis, Numerical integration using Rys polynomials. J. Comput. Phys. **21**, 144–165 (1976)
16. A.M. Köster, R. Flores-Moreno, J.U. Reveles, Efficient and reliable numerical integration of exchange correlation energies and potentials. J. Chem. Phys. **121**, 681–690 (2004)
17. V.I. Lebedev, Spherical quadrature formulas exact to orders 25–29. Sib. Math. Zh. **18**, 132–142 (1977)
18. R. Lindh, P .A. Malmqvist, L. Gagliardi, Molecular integrals by numerical quadrature. I. Radial integrals. Theor. Chem. Acc. **106**, 178–187 (2001)
19. R. Lindh, U. Ryu, B. Liu, The reduced multiplication scheme of the Rys quadrature and new recurrence relations for auxiliary function based two-electron integral evaluation. J. Chem. Phys. **95**, 5889–5897 (1991)
20. B.A. Mamedov, H. Koç, Calculation of two-center overlap integral in molecular coordinate system over Slater type orbital using L"owdin α-radial and Guseinov rotation-angular functions. J. Math. Chem. **44**, 365–372 (2008)
21. J.M.L. Martin, C.W. Bauschlicher Jr., A. Ricca, On the integration accuracy in molecular density theory calculation using Gaussian basis sets. Comput. Phys. Commun. **133**, 189–201 (2001)

22. M. Mitani, An application of double exponential formula to radial quadrature grid in density functional calculation. Theor. Chem. Acc. **130**, 645–669 (2011)
23. D.A. Morales, On the evaluation of integrals with Coulomb Sturmian radial functions. J. Math. Chem. **54**, 682–689 (2016)
24. M.E. Mura, P.J. Knowles, Improved radial grids for quadrature in molecular density-functional calculations. J. Chem. Phys. **104**, 9848–9858 (1996)
25. C.W. Murray, N.C. Handy, G.L. Lamming, Quadrature schemes for integrals of density functional theory. Mol. Phys. **78**, 997–1014 (1993)
26. R.M. Parrish, E.G. Hohenstein, T.J. Martnez, C.D. Sherrill, Discrete variable representation in electronic structure theory: quadrature grids for least-squares tensor hypercontraction. J. Chem. Phys. **138**, 194107 (2013)
27. J.M. Pérez-Jordá, A.D. Becke, E. San-Fabiń, Automatic numerical integration techniques for polyatomic molecules. J. Chem. Phys. **100**, 6520–6534 (1994)
28. S. Reine, T. Helgaker, R. Lindh, Multi-electron integrals. WIREs Comput. Mol. Sci. **2**, 290–303 (2012)
29. J.I. Rodriguez, D.C. Thompson, P.W. Ayers, A.M. Köster, Numerical integration of exchange-correlation energies and potential using transformed sparse grids. J. Chem. Phys. **126**, 224103 (2008)
30. K. Shah, Asymptotic solution of Fokker–Planck equation for plasmas in Paul traps. Phys. Plasmas **17**, 054501 (2010)
31. J. Shen, L.L. Wang, Some recent advances on spectral methods for unbounded domains. Commun. Comput. Phys. **5**, 195–241 (2009)
32. C.D. Sherrill, Frontiers in electronic structure theory. J. Chem. Phys. **132**, 110902 (2010)
33. B. Shizgal, A Gaussian quadrature procedure for the use in the solution of the Boltzmann equation and related problems. J. Comput. Phys. **41**, 309–328 (1981)
34. B. Shizgal, A novel Rys quadrature algorithm for use in the calculation of electron repulsion integrals. Comput. Theor. Chem. **2015**, 178–184 (1074)
35. B. Shizgal, *Spectral Methods in Chemistry and Physics; Application to Kinetic Theory and Quantum Mechanics* (Springer, New York, 2015)
36. R. Sospedra-Alfonso, B.D. Shizgal, Kullback-Leibler entropy in the electron distribution shape relaxation for electron-atom thermalization. Phys. Rev. E **84**, 041202 (2011)
37. R. Sospedra-Alfonso, B.D. Shizgal, Energy and shape relaxation in binary atomic systems with realistic quantum cross sections. J. Chem. Phys. **139**, 044113 (2013)
38. O. Treutler, R. Ahlrichs, Efficient molecular numerical integration schemes. J. Chem. Phys. **102**, 346–354 (1995)
39. T. Tsuneda, *Density Functional Theory in Quantum Chemistry* (Springer, New York, 2014)